Optical, Structural and Morphological Evaluation of Electrodeposited Chromium Selenide (CRSE) Thin Films

Ifunanya Peace Okeke[1]*, Azubuike Josiah Ekpunobi [2], Okafor Chiedozie Emmanuel[2], Onyewuchi Pascal Chibuke[1]

[1]Department of Physics Education, Federal college of education (Technical), Umunze, Nigeria

[2]Department of Physics and Industrial Physics, Nnamdi Azikiwe University Awka, Nigeria

***Corresponding Author**

DOI: https://doi.org/10.51244/IJRSI.2026.1303000022

Received: 08 March 2026; Accepted: 14 March 2026; Published: 25 March 2026

ABSTRACT

Chromium selenide (CrSe) thin films was successfully deposited on fluorine-doped tin oxide (FTO) conducting substrates using an electrodeposition technique. The films exhibited thicknesses ranging from 71.22–166.17 nm, with thickness increasing progressively with deposition potential due to enhanced ionic transport and accelerated film nucleation. Optical characterization revealed absorbance values between 6.16–30.39%, which increased with deposition potential and decreased with increasing wavelength. Transmittance values ranged from 49.67–88.90%, showing a reverse trend, decreasing with higher deposition potentials and increasing with wavelength. The CrSe films showed low reflectance across the UV–NIR range, with values between 5.99–19.94%, and maxima occurring in the UV region. The refractive index values ranged from 1.63–2.64, decreasing with wavelength but rising with deposition potential. Extinction coefficient values were between 9.50×10^{-2} – 2.01×10^{-1}, while optical conductivity ranged from 6.42×10^{13} – 50.48×10^{13} s^{-1}.Tauc analysis revealed that the energy bandgap varied with deposition potential, ranging from 3.00–3.25 eV, confirming CrSe as a wide bandgap semiconducting material suitable for optoelectronic and photovoltaic applications. XRD analysis confirmed hexagonal phase CrSe, with crystallite sizes of 30.780–33.455 nm, dislocation densities of 9.050×10^{14} – 1.092×10^{15} lines/m², and microstrains of 3.09×10^{-3} – 8.46×10^{-3}. SEM micrographs showed surfaces composed of tiny agglomerated particles of irregular shapes and sizes, while EDS analysis confirmed the elemental presence of chromium and selenium. These results demonstrate that electrodeposited CrSe thin films possess desirable structural and optical characteristics for use in optoelectronic, photovoltaic, and spintronic applications.

Key words: Chromium Selenide, Semiconductors, Electrodeposition, Photovoltaics, Bandgaps

Graphical abstract

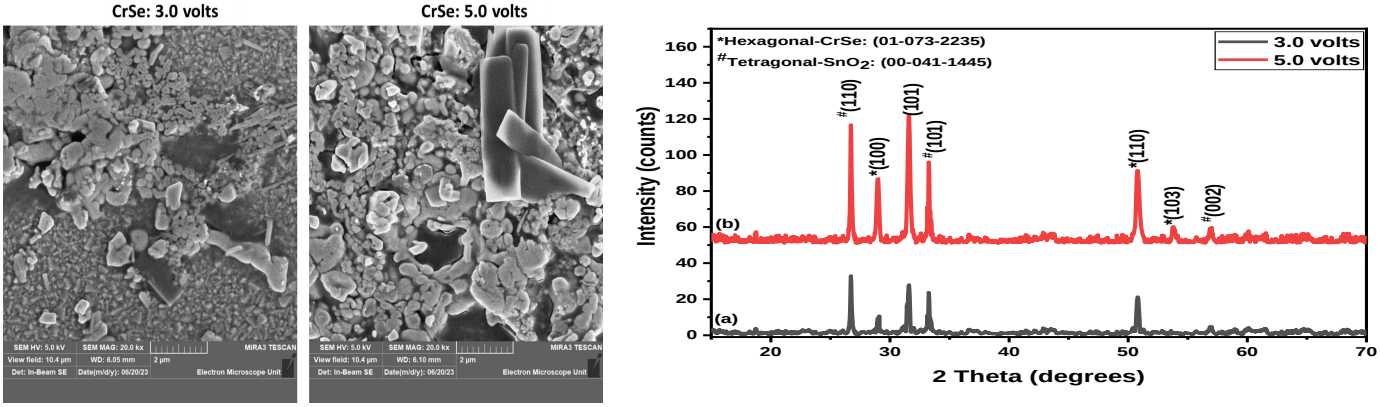

ISSN No. 2321-2705 | DOI: 10.51244/IJRSI |Volume XIII Issue III March 2026

INTRODUCTION

Chromium selenide (CrSe) belongs to the broad class of transition metal chalcogenides (TMCs), a group of compounds widely explored for their diverse magnetic, optical, and electronic functionalities. As an antiferromagnetic semiconductor, CrSe exhibits a Néel temperature between 94–320 K and undergoes a structural transformation from the NiAs-type to the MnP-type lattice near 575 K due to the Jahn–Teller effect [1]. Such transitions influence its electronic band structure and give rise to anomalies in conductivity and magnetic susceptibility—traits that make CrSe an important material for next-generation optoelectronic and spintronic devices. [13].

Transition metal selenides continue to gain prominence in solar energy conversion, nanoelectronics, photodetectors, sensors, and supercapacitor technologies due to their tunable bandgaps, high absorption coefficients, and stable crystal frameworks. [15].

Recent studies have demonstrated the versatility of these materials in multilayer and engineered heterostructures, where their optoelectronic responses can be modulated by altering thickness, deposition parameters, or lattice arrangements. Within this class, chromium selenide has remained particularly attractive because of its ability to form stable thin films, its semiconducting behavior, and its magnetic ordering linked to Cr^{2+}/Cr^{3+} electronic configurations. [28].

Electrodeposition has emerged as a key technique for synthesizing binary selenide thin films (including FeSe, CrSe, and FeSe/CrSe systems) because it offers low-temperature processing, affordability, and precise control over stoichiometry, nucleation, and film thickness [2]. The article by [16] highlights the strengths of this technique, noting its ability to produce uniform thin films using a three-electrode configuration typically involving an FTO working electrode, a platinum counter electrode, and an Ag/AgCl reference electrode. This method facilitates layer-by-layer growth, which is essential for designing complex architectures such as superlattices and multilayer structures. In addition, electrodeposition provides a platform for tuning film properties via adjustable deposition potentials, as demonstrated by the variation in morphology, crystallinity, and optical behavior of FeSe/CrSe superlattice films fabricated at potentials from 3.0 to 5.0 V .

With the growing interest in wide-bandgap semiconductors for optoelectronic applications, chromium selenide thin films offer a promising platform for device engineering[4]. Their ability to exhibit tunable bandgaps (as low as 2.60 eV in the superlattice system), low reflectance, and strong UV absorption makes them viable materials for UV shielding, antireflective coatings, and photodetection technologies. The structural integrity and layered stability of CrSe further enhance its suitability for integration into multilayer systems and superlattice architectures. [13]

Consequently, this work focuses exclusively on the fabrication and characterization of CrSe thin films deposited on FTO substrates using electrodeposition method. The aim is to deepen understanding of the intrinsic structural, optical, and morphological properties of chromium selenide, independent of its behavior in multilayer structures, and to explore its potential for future semiconductor, photovoltaic, and nano-optoelectronic applications.

MATERIALS AND METHODS

Reagents

Reagents used for electrodeposition of chromium selenide (CrSe) were chromium (III) trioxonitrate (V) nanohydrate as precursor for chromium ion, selenium (IV) oxide as precursor for selenium ion, sodium sulphate as supporting electrolyte and distilled water was used as solvent.

Apparatus

The following apparatus were used during the experiment; Beakers (l00ml): used for mixing solutions.

ISSN No. 2321-2705 | DOI: 10.51244/IJRSI |Volume XIII Issue III March 2026

Fluorine doped tin oxide (FTO) glass slide ($17\Omega/sq$): this is used as the substrates or working electrode. Electronic compact scale (Atom: model 110C, capacity – 750 g, accuracy - 0.01g): used for the determination of the weight of reagents. Magnetic stirrer hotplate (Labscience 85 – 2): used for stirring the solutions. DC Power Supply: served as a source of electric energy (potential difference). Digital multimeters (DT9201A CE and Mastech: MY60): for measuring current and voltage. Platinum rod: used as counter electrode. Ag/AgCl electrode: used as reference electrode. Ultrasonic bath: for degreasing the substrates and electrical oven used for drying.

Material Preparation

The reagents are of analytical grade and used without further purification or modification. The desired molar solutions of the reagents were prepared and used for the depositions. 0.10 M of chromium (III) trioxonitrate (V) nanohydrate was prepared by dissolving 10.00 g of the compound in 250 ml of distilled water. 0.10 M of SeO_2 was prepared by dissolving 2.77 g in 250 ml of distilled water. 0.05 M of sodium sulphate (Na_2SO_4) which was used as supporting electrolyte was prepared by dissolving 8.06 g in 500 ml of doubled distilled water.

Substrate Pre-treatment

The cleaning process for preparing FTO (Fluorine-doped Tin Oxide) glass substrates for electrodeposition of films involves several crucial steps. Initially, the FTO glass slides were meticulously cleaned with a detergent solution to eliminate any surface dust, dirt, or contaminants that could hinder the subsequent stages of preparation. Following this, the slides are immersed in acetone for a period of 10 minutes to effectively degrease the surface, removing any residual oils or greases that might interfere with film adhesion. Subsequently, the substrates undergo ultrasonic treatment in an ultrasonic bath for 10 minutes. This step employs high-frequency vibrations to dislodge and eliminate any remaining particles or contaminants adhering to the substrate. Finally, to ensure complete dryness, the substrates are placed in an electric oven and heated to 100 ℃ for 10 minutes, ensuring the removal of any lingering moisture that could negatively affect the electrodeposition process and the films adhesion.

Electrodeposition of CrSe thin films

Figure 1 depicts the electrodeposition setup, which includes the electrolyte, power supply unit, and the electrodes. The electrodeposition setup utilized in this work is identical to the one employed by [33], as illustrated in Figure 1. The setup consisted of a three-electrode electrodeposition configuration for deposition of thin films on a conducting substrate. The conducting substrate, FTO (Fluorine-doped Tin Oxide) glass, served as the working electrode, functioning as the cathode. A platinum electrode was employed as the counter electrode which served as the anode. An Ag/AgCl electrode was utilized as the reference electrode. The Dazheng digital DC-power supply unit (PS-1502A) model served as the energy source for the electrodeposition setup. Two digital multimeters (DT9201A CE, and Mastech MY60) were incorporated into the setup to measure potential difference and current, respectively. To initiate the electrodeposition of chromuim selenide (CrSe) thin films onto an FTO substrate, a well-mixed aqueous electrolytic bath was formulated. This bath consisted of 15 ml of 0.20 M chromium (III) trioxonitrate (V) nanohydrate and 15 ml of 0.10 M selenium dioxide, mixed thoroughly with magnetic stirrer for 5 minutes. Following this, 5 ml of 0.05 M Na_2SO_4 was introduced, and the resulting solution underwent an additional 5 minutes of magnetic stirring. Subsequently, the three electrodes were immersed into the electrolytic bath, and a consistent potential of 3.0 volts was constantly maintained for precisely 2 minutes. This controlled electrochemical process culminated in the formation of CrSe thin film deposit, which was subsequently subjected to a thermal treatment at 100 ℃ for a duration of 20 minutes to optimize its properties.

ISSN No. 2321-2705 | DOI: 10.51244/IJRSI |Volume XIII Issue III March 2026

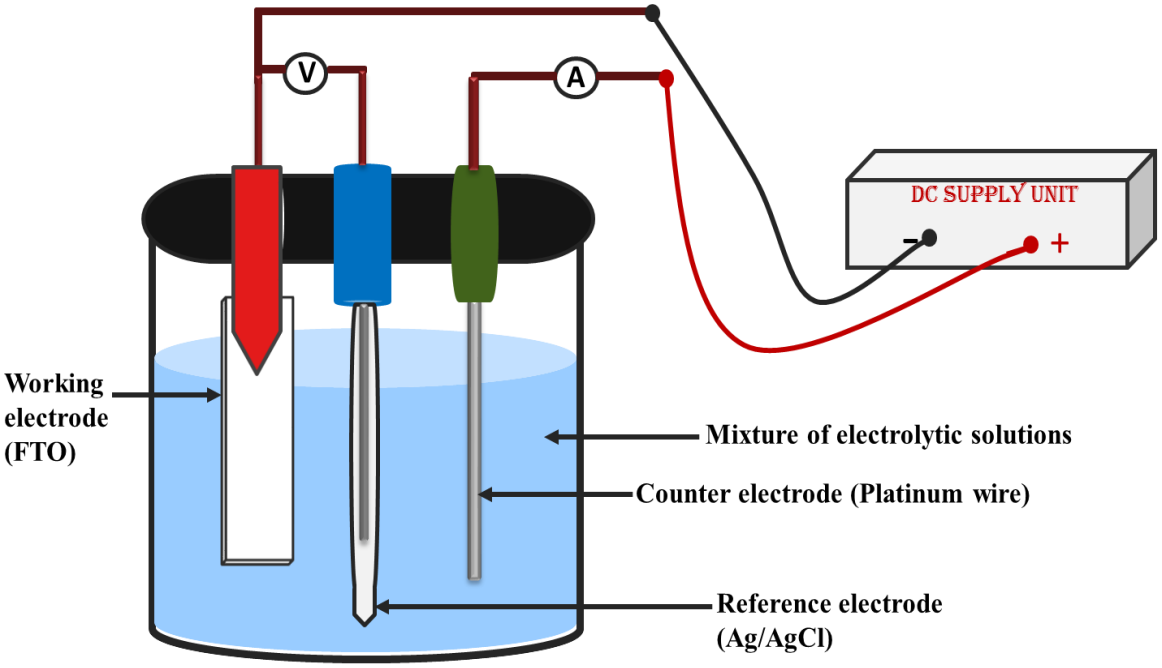

Figure 1: Schematic diagram of the electrodeposition experimental set up (Okoli *et al.*, 2022)

RESULTS AND DISCUSSION

Optical properties of CrSe thin films Absorbance values of the films were measured with UV-VIS spectrophotometer within the wavelength of 300 nm to 1100 nm. Other properties such as transmittances, reflectance, refractive index, extinction coefficient, and energy band gap were evaluated according to expressions as described below. Transmittance of the film was evaluated using Equation (1) as given by [6-8].

$$T = 10^{-A} \quad (1)$$

Reflectance was obtained using the expression in equation (2) as given by [4-5,20].

$$R = 1 - [T \cdot \exp(A)]^{1/2} \quad (2)$$

The absorption coefficient (α) was calculated from the transmittance values using Equation (3) as given by [27,1].

$$\alpha = 1/t \ \text{In} \ (1/T). \quad (3)$$

Where, t is film thickness obtained using gravimetric method as described by [27, 8, 17].

Extinction coefficient was obtained using equation (4) as given by [9, 5,22].

$$k = \frac{\alpha \lambda}{4\pi} \quad (4)$$

Refractive indices of the films were calculated using Equation (5) as given by [18,5]:

$$\eta = \frac{1+R}{1-R} + \sqrt{\frac{4R}{1-R} - K^2} \quad (5)$$

The energy band gap was estimated using Tauc's model of equation (6) as given by [31, 11, 21]:

ISSN No. 2321-2705 | DOI: 10.51244/IJRSI |Volume XIII Issue III March 2026

$$(\alpha hv)^{n} = (hv - Eg) \quad (6)$$

Where, β is a constant, n = 2 for direct band gap. The energy band gaps of the films were obtained by extrapolating the straight portion of the plot of $(\alpha hv)^{2}$ against the photon energy (hv) at

$(\alpha hv)^{2} = 0$.

Figure 2 displays the absorbance graph plotted against wavelength for CrSe thin films electrodeposited at various deposition potentials. The results reveal a consistent trend of decreasing absorbance as photon wavelength increases. Interestingly, superlattice films demonstrate an inverse correlation between absorbance and deposition potential, with the 5.0-volt deposition registering the highest absorbance at 80.91% at 300 nm. In contrast, the 3.0-volt thin film exhibits a decline in absorbance from 27.60% at 300 nm to 20.57% at 400 nm, followed by a further decrease to 12.11% at 700 nm and 11.70% at 1000 nm in the near-infrared (NIR) range. A similar pattern is observed for films deposited at 3.5, 4.0, and 4.5 volts, with decreasing absorbance as wavelength increases, indicating the critical role of deposition potential in tailoring absorbance characteristics for specific applications. Due to the high absorbing nature of these films within UV region, they could be used in antireflective window coating in tropical regions of the world to shield harmful effect of UV radiations. Similar trend of increase in absorbance as deposition potential increases was obtained by [11, 21,20].

Figure 4 shows the graph of transmittance plotted against wavelength for FCrSe thin films deposited at different deposited potential. Transmittance values increase with longer wavelengths, while they decrease as the deposition potential rises. This reduction in transmittance at higher deposition potentials results from increased photon energy absorption due to thicker films.

For instance, Chromium selenide thin film deposited at 4.0 volts has transmittance values that increased from 62.48% at 300 nm to 69.64 % at 400 nm. The values increased further to 77.02% at 700 nm and further increased to 76.20% at 1000 nm. Chromium selenide thin film deposited at 4.5 volts has transmittance values that increased from 55.49 at 300 nm to 64.14% at 400 nm. It increased further to 75.29% at 700 nm and up to 75.36% at 1000 nm. Chromium selenide thin film deposited at 5 volts has transmittance values that increased from 49.67% at 300 nm to 55.00% at 400 nm. It increased further to 65.66% at 700 nm and further to 68.81% at 1000 nm. Similar decrease in transmittance as applied voltage increases has been reported by [3]

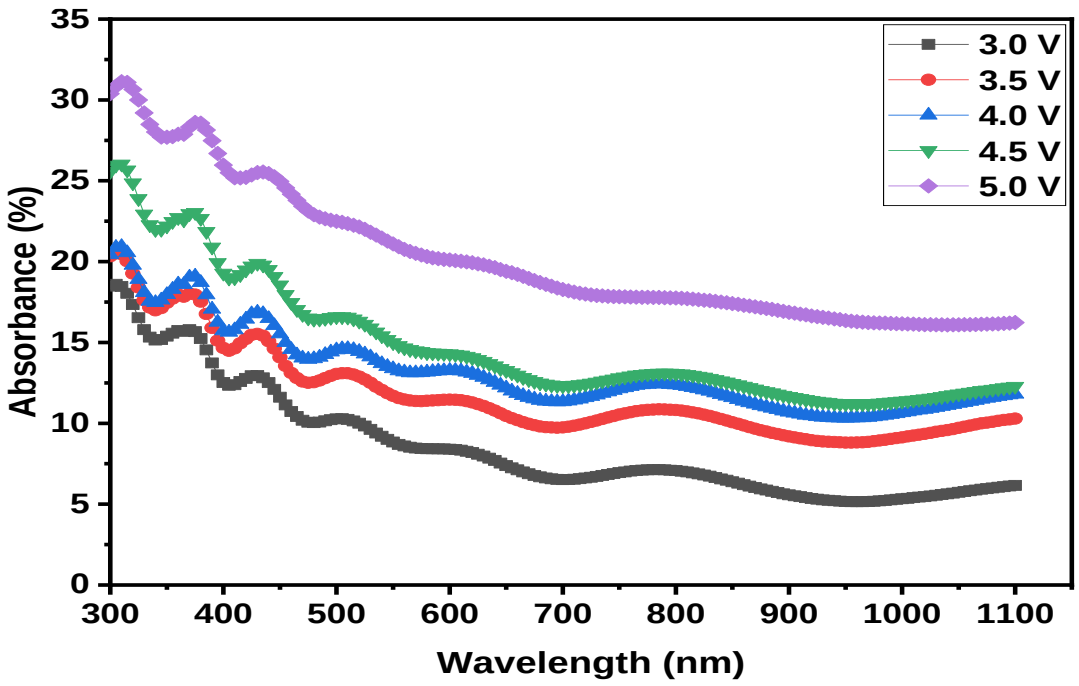

Figure 2: Plot of absorbance against wavelength for chromium selenide thin films deposited at different

ISSN No. 2321-2705 | DOI: 10.51244/IJRSI |Volume XIII Issue III March 2026

deposition potential

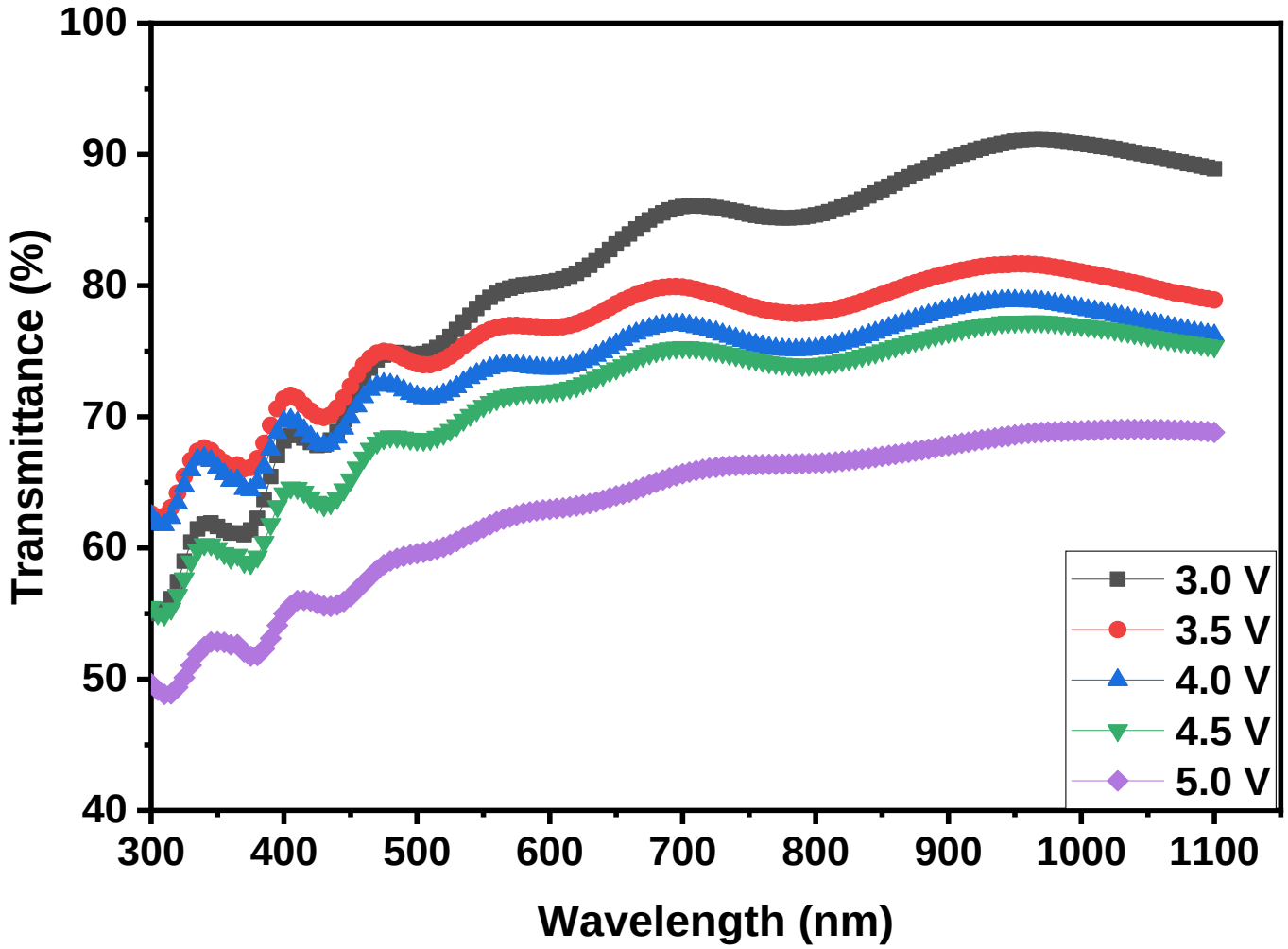

Figure 3: Plot of transmittance against wavelength chromium selenide thin films deposited at different deposition potential

Figure 4 shows the graph of reflectance plotted against wavelength for CrSe thin films deposited at different values of deposition potential. Reflectance values of deposited chromium selenide were found to be low. From the graph, reflectance values of the thin films were found to decrease as wavelength increase. Also, reflectance of the CrSe thin films were found to increase as deposition potentials increases. Reflectance peaks were observed within UV and some part of the VIS regions. Chromium selenide thin film deposited at 3.0 volts has reflectance values that ranged between 19.00% and 5.99%. Chromium selenide thin film deposited at 3.5 volts has reflectance values that ranged between 17.05% and 10.81%. Chromium selenide thin film deposited at 4.0 volts has reflectance values that ranged between 17.10% and 12.00%. Chromium selenide thin film deposited at 4.5 volts has reflectance values that ranged between 18.93% and 12.36%. Chromium selenide thin film deposited at 5.0 volts has reflectance values that ranged between 19.94% and 14.95%.

Figure 5 demonstrates the graph of refractive index plotted against wavelength for CrSe thin films deposited at different values of deposition potential. Refractive index values of deposited chromium selenide were found to be low. From the graph, refractive index values of the thin films were found to decrease as wavelength increase. Also, refractive index of the CrSe thin films were found to increase as deposition potentials increases. Refractive index peaks were observed within UV and some part of the VIS regions. Chromium selenide thin film deposited at 3.0 volts has refractive index values that ranged between 2.53 and 1.63. Chromium selenide thin film deposited at 3.5 volts has refractive index values that ranged between 2.40 and 1.95. Chromium selenide thin film deposited at 4.0 volts has refractive index values that ranged between 2.41 and 2.03.

ISSN No. 2321-2705 | DOI: 10.51244/IJRSI |Volume XIII Issue III March 2026

Chromium selenide thin film deposited at 4.5 volts has refractive index values that ranged between 2.54 and 2.06. Chromium selenide thin film deposited at 5.0 volts has refractive index values that ranged between 2.61 and 2.24.

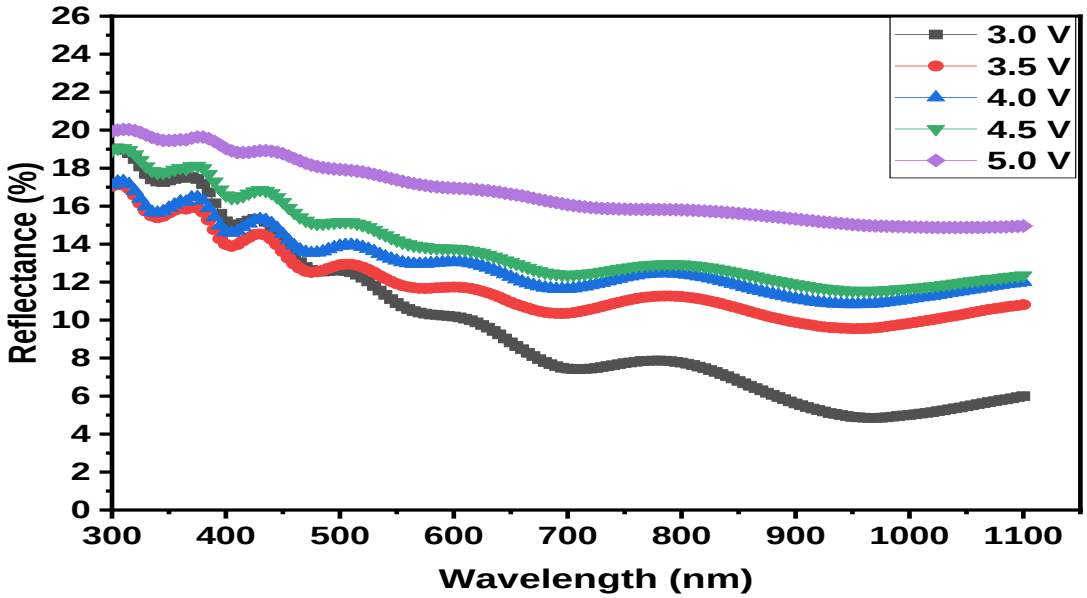

Figure 4: Plot of reflectance against wavelength for chromium selenide thin films deposited at different deposition potential

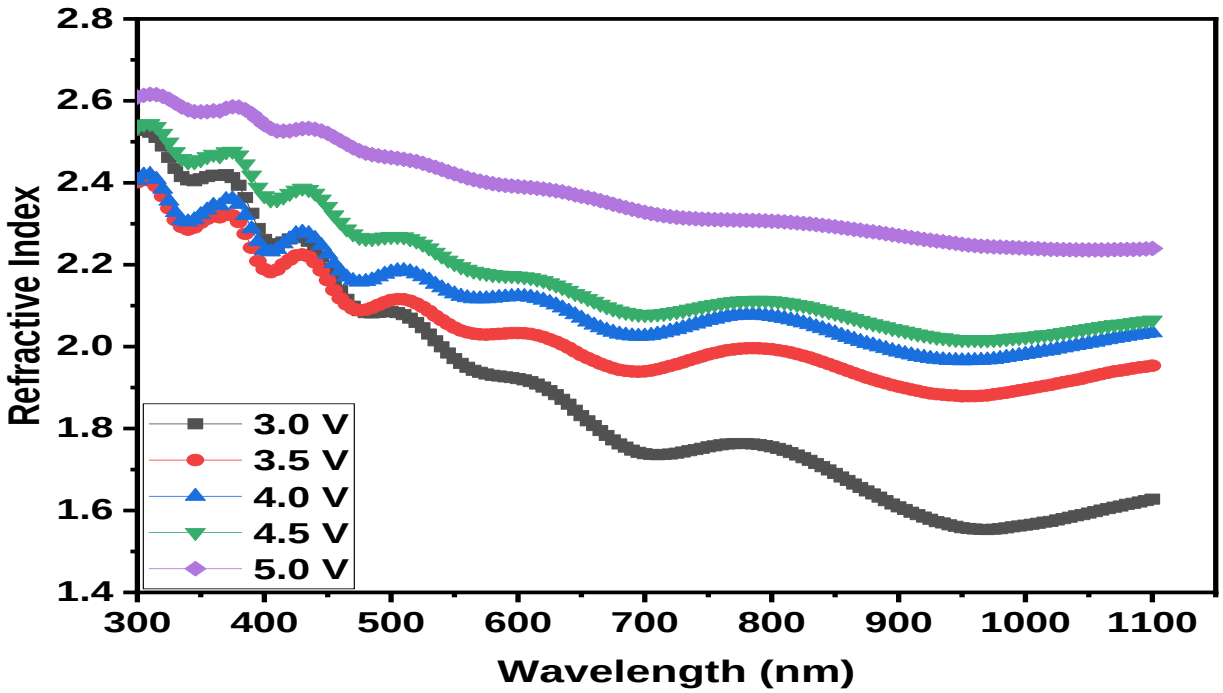

Figure 5: Plot of refractive index against wavelength for chromium selenide thin films deposited at different deposition potential

Figure 6 illustrates the graph of extinction coefficient of CrSe thin films at varying deposition potential. Extinction coefficient values of the films were found to increase as wavelength increases except for CrSe film deposited at potential of 3.0 volts that showed decrease in extinction coefficient within UV and VIS regions and increase within NIR at wavelength range of 950 – 1100 nm. Also, no linear relationship was observed between deposition potential and extinction coefficient of the deposited CrSe thin films. Chromium selenide

ISSN No. 2321-2705 | DOI: 10.51244/IJRSI |Volume XIII Issue III March 2026

thin films deposited at 3.0 volts, 3.5 volts, 4.0 volts, 4.5 volts and 5.0 volts have extinction coefficient values that ranged from $2.00 \times 10^{-1} - 1.18 \times 10^{-1}$, $1.94 \times 10^{-1} - 1.01 \times 10^{-1}$, $2.01 \times 10^{-1} - 9.50 \times 10^{-2}$, $1.74 \times 10^{-1} - 9.90 \times 10^{-2}$ and $1.97 \times 10^{-1} - 1.01 \times 10^{-1}$ respectively. These range of extinction coefficient values confirmed that these films are good for absorber layer of thin film solar cells.

Figure 7 shows the plot of $(\alpha hv)^2$ against photon energy for CrSe thin films deposited at different deposition potentials. From the plot, energy band gap of the films were estimated by extrapolation of the straight portion of the graph along the photon energy axis, where $(\alpha hv)\ 2 = 0$. Energy band gap of 3.25 eV was obtained for CrSe thin film deposited at 3.0 volts while band gap values of 3.20 eV, 3.10 eV, 3.10 eV, and 3.00 eV were obtained for CrSe thin films deposited at 3.5 volts, 4.0 volts, 4.5 volts, and 5.0 volts respectively.

The result showed a decrease in energy band gap of films as deposition potential increases. This confirmed the likelihood of tuning energy band gap of CrSe by varying the deposition potential. Similar effect of deposition potential on the band gap of thin film materials had been reported by [13,14, 26]. The increase in deposition potential gives rise to increase in the films thickness which is likely to be due to quantum confinement effect.

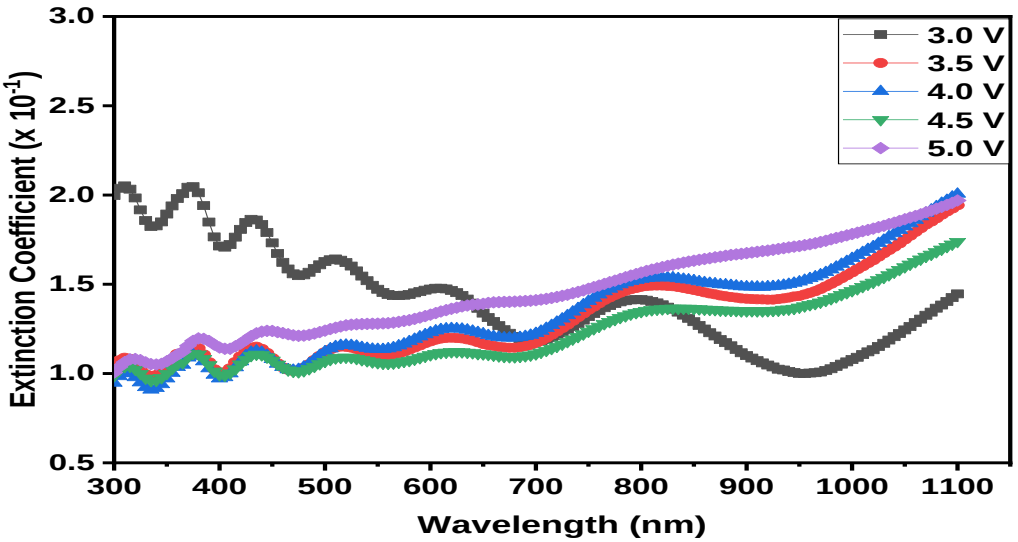

Figure 6: Plot of extinction coefficient against wavelength for chromium selenide thin films deposited at different deposition potential

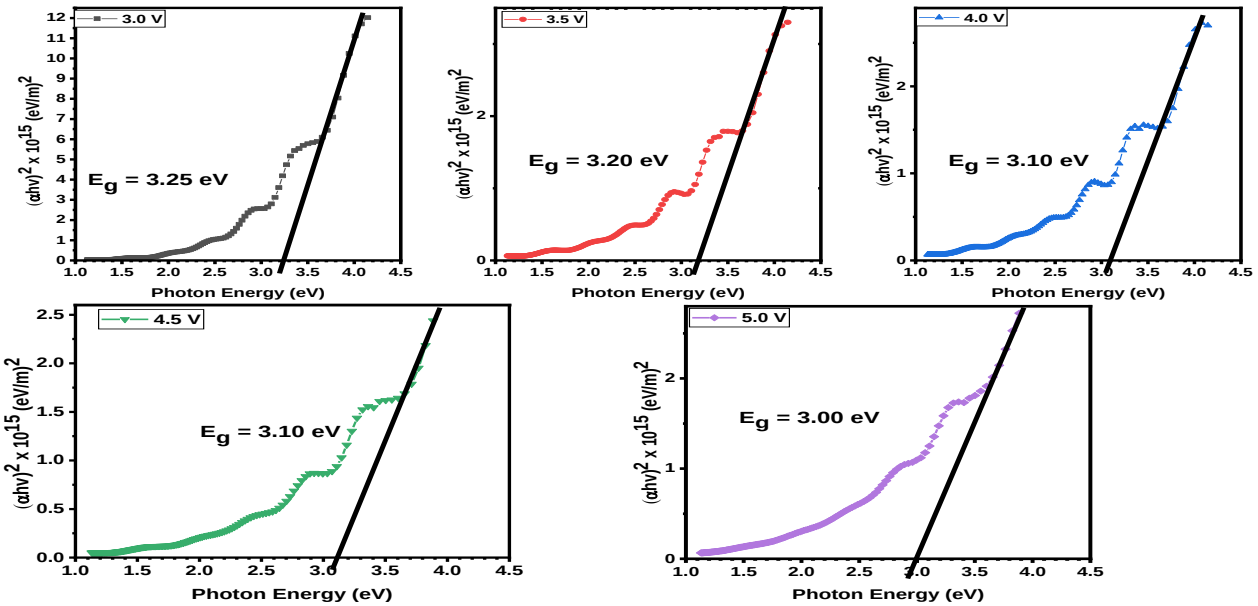

ISSN No. 2321-2705 | DOI: 10.51244/IJRSI |Volume XIII Issue III March 2026

Figure 7: Plot of $(\alpha h\nu)^2$ against photon energy for chromium selenide thin films deposited at different deposition potential

Morphological study of CrSe thin films

Figure 8 displays SEM images of CrSe thin films deposited at deposition 3.0 volts and 5.0 volts. These images reveal agglomerated nanoparticles with varying sizes and shapes on the film surfaces. Particle agglomeration intensifies with higher deposition potential, indicative of a direct electrochemical influence on film morphology. Notably, rectangular plate-like particles are observed in the CrSe thin film at 5.0 volts. Quantitative analysis confirms that the average particle size increases from 60.41 nm at 3.0 volts to 68.29 nm at 5.0 volts, aligning with visual observations. These results highlight the correlation between deposition potential and particle behavior in thin film growth. The observed morphological changes suggest a shift in growth mechanism as deposition potential rises. This interplay underscores the significance of electrochemical conditions in shaping the microstructure of CrSe thin films. Such insights hold relevance for tailoring thin film properties for diverse applications. In essence, the SEM images and quantitative analysis provide comprehensive insights into the intricate relationship between deposition potential and the resulting characteristics of CrSe thin films.

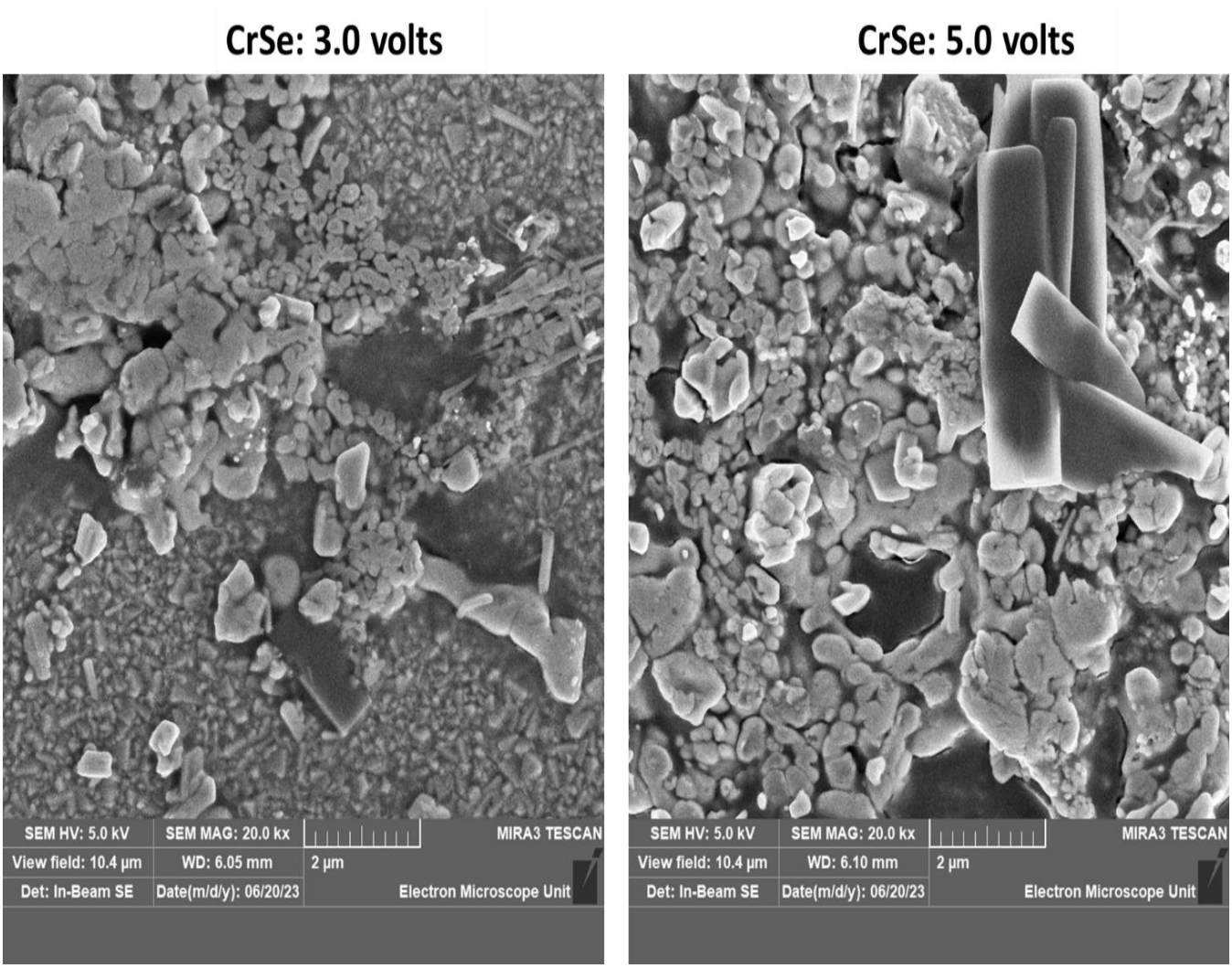

Figure 8: SEM image of CrSe thin films deposited at 3.0 volts and 5.0 volts

Compositional study of FeSe/CrSe superlattice thin films

Figure 9 shows the EDS spectrum of CrSe thin film deposited at 3.0 and 5.0 volts. The EDS spectrum confirmed the presence of chromium (Cr) and selenium (Se). Other elements such as oxygen (O), carbon (C),

ISSN No. 2321-2705 | DOI: 10.51244/IJRSI |Volume XIII Issue III March 2026

silicon (Si) and tin (Sn) were found to be present in the sample. These elements are attributed to constituents of the substrate used for the deposition. Atomic percentage of chromium were found to increase slightly as deposition potential increased from 3.0 volts to 5.0 volts while atomic percentage of Se was found to decrease as deposition potential increased from 3.0 volts to 5.0 volts.

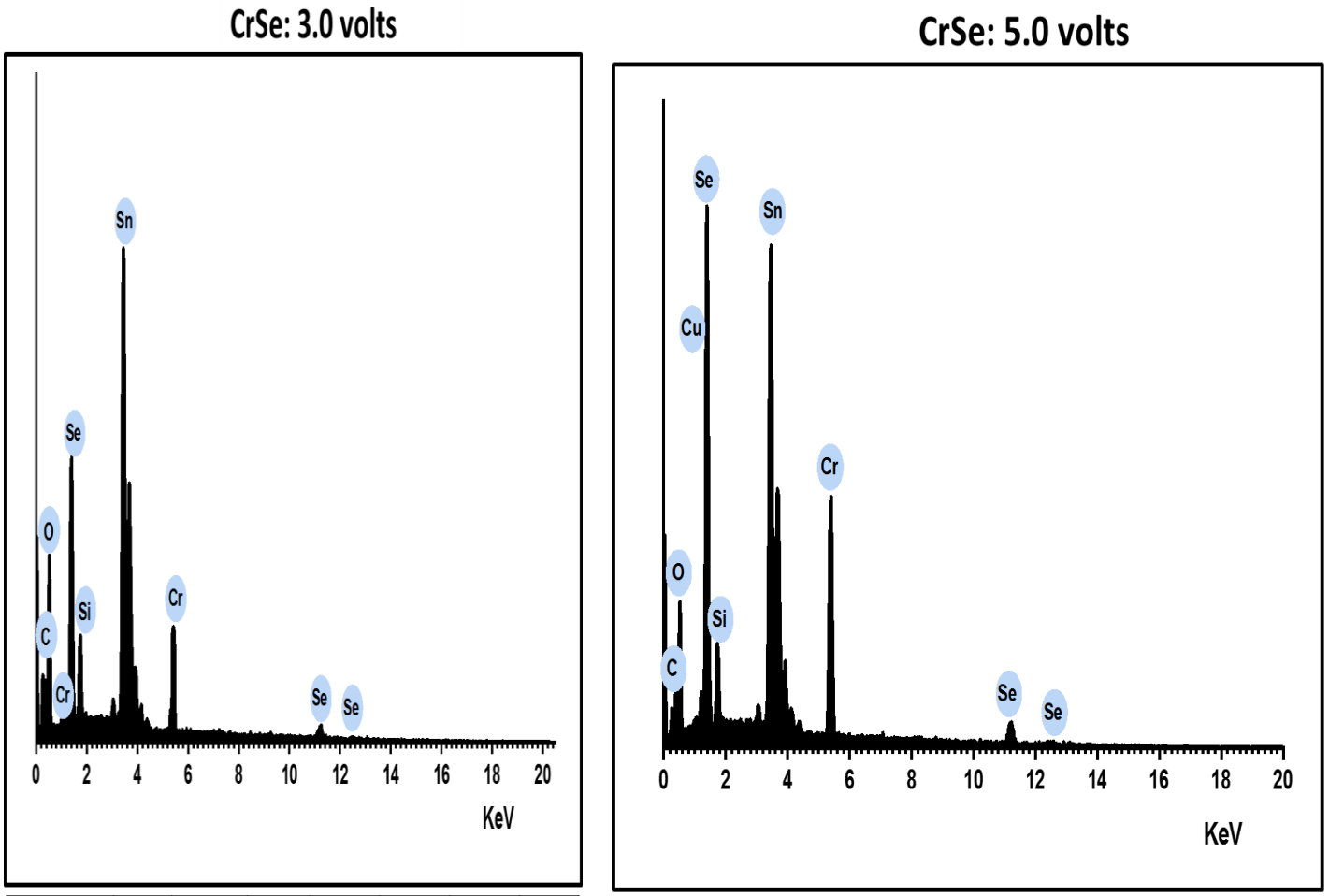

Elements	C	O	Si	Se	Cr	Sn	Total
Atomic %	3.58	11.59	1.93	28.96	23.5	30.44	100

Elements	C	O	Si	Se	Cr	Sn	Total
Atomic %	3.05	11.34	1.82	29.14	25.40	27.25	100

Figure 9: EDS spectrum of CrSe thin films deposited at 3.0 and 5.0 volts

Figure 10 shows the x-ray diffraction pattern of electrodeposited CrSe thin films deposited at deposition potential of 3.0 and 5.0 volts. The result shows that the fabricated CrSe thin films are of hexagonal crystal phase belonging to the JCPDS file number (01-073-2235). Peaks corresponding to peaks of this standard JCPDS file were observed for the films. Three corresponding peaks were observed for CrSe thin film deposited at 3.0 volts while 4 corresponding peaks were observed for films deposited at 5.0 volts. Two additional peaks at 26.721 ° and 33.381 ° belonging to SnO_2 with JCPDS file number (00-041-1445) were observed in the films. The existence of these two peaks is as a result of the nature of the substrate used for the deposition.

Table 1 shows the structural parameters of the deposited CrSe thin films. In all the thin film samples preferential orientation was observed at [101] plane. The structural parameters such as observed 2 theta angles, observed d – spacings, full width half maximum (FWHM), miller indices (hkl), and crystallite sizes of the synthesized CrSe thin films are presented in table 4.4. The average crystallite sizes of $30.780\ nm$ and $33.455\ nm$ were obtained for CrSe thin films deposited 3.0 and 5.0 volts. Dislocation densities of the thin films were found to be 1.092×10^{15} lines/m^2 and 0.905×10^{15} lines/m^2 while microstrain were found to be 3.909×10^{-3} and 3.18×10^{-3} respectively. The structural results show that crystallite size of the deposited

ISSN No. 2321-2705 | DOI: 10.51244/IJRSI |Volume XIII Issue III March 2026

CrSe thin films increased as deposition potential increased from 3.0 to 5.0 volts. Also, dislocation density and microstrain of the films were found to decrease as deposition potential increased from 3.0 to 5.0 volts. Same hexagonal phase of CrSe have been obtained by [10,12] while [23-25] obtained hexagonal structure corresponding to JCPDS file number of 98-062-6908.

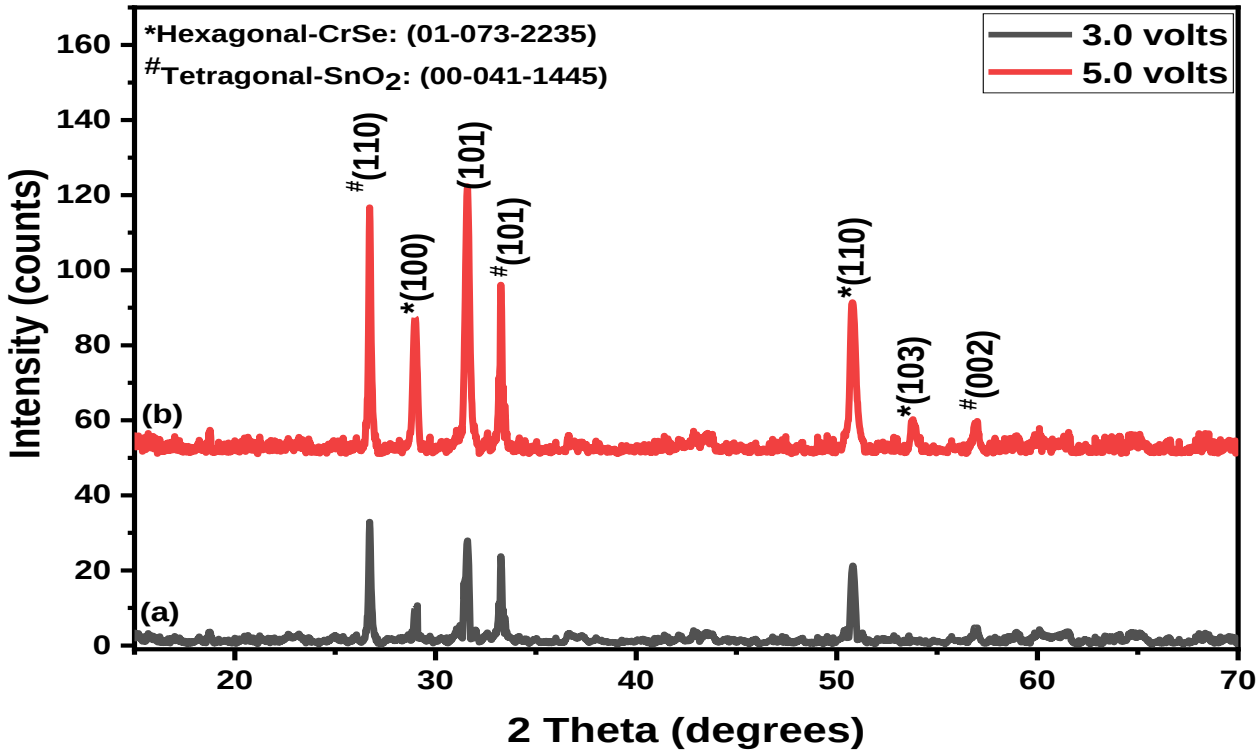

Figure 10: X-ray spectra of CrSe thin films deposited at (a) 3.0 volts and (b) 5.0 volts

Table 1: Crystal structural properties of CrSe thin films formed at 3.0 volts and 5.0 volts with lattice constants of 3.71 Å, 3.71 Å and 6.03 Å.

Sample	2θ (°)	D – spacing (Å)	[hkl]	FWHM (°)	Crystallite Size (nm)	$\delta \times 10^{15}$ lines/m^2	$\varepsilon \times 10^{-3}$
	Observed	Observed					
3.0 volts	28.989	3.078	100	0.289	29.701	1.134	4.870
	31.567	2.832	101	0.244	35.313	0.802	3.769
	50.803	1.796	110	0.336	27.326	1.339	3.089
Average					**30.780**	**1.092**	**3.909**
5.0 volts	28.98	3.079	100	0.249	34.39	0.846	4.207
	31.59	2.830	101	0.267	32.288	0.959	4.119
	50.807	1.796	110	0.300	30.599	1.068	2.758
	53.821	1.702	**103**	0.255	36.542	0.749	2.189
	Average				**33.455**	**0.905**	**3.318**

CONCLUSION

Chromium selenide thin films were successfully electrodeposited onto conducting substrates (FTO: fluorine-doped tin oxide). Extensive analyses encompassing optical, structural, morphological, and compositional aspects were conducted. The absorbance spectra showed gradual decrease in absorbance as photon wavelength increases. The CrSe film deposited at 3.0 volts exhibited absorbance values of 18.0% at 300 nm, 13.1% at 400

nm, 7.5% at 700 nm, and 5.1% at 1000 nm. In contrast, the thin film deposited at 5.0 volts displayed the highest absorbance, with a value of 32.1% at 300 nm. Transmittance values decreased as deposition potential increased and increased with longer wavelengths. At 3.0 volts, transmittance ranged from 61.15% at 300 nm to 90.19% at 1000 nm, while at 5.0 volts, transmittance values followed a similar trend, emphasizing the wavelength-dependent and potentialdependent behavior of transmittance CrSe thin films. These films displayed consistently low reflectance values across all studied wavelength regions, with the highest reflectance found in the UV region. Refractive index values decreased with longer wavelengths and increased with higher deposition potentials. No linear relationship was found for the extinction coefficient variation with the number of deposition potentials. Energy bandgap values decreased from 3.25-3.0 eV as deposition potential increased from 3.0 to 5.0 volts. These energy band gap values indicate that CrSe thin films are wide-bandgap semiconductors suitable for optoelectronic applications. Structural analysis revealed increasing crystallite sizes from 29.701-36.542 nm as deposition potential increases. Dislocation density was found to decrease from 1.134×10^{15} - 0.905×10^{15} lines/m^2 while microstrain decreased from 4.870×10^{-3} - 2.189×10^{-3} as deposition potential increases. Surface morphology studies revealed diverse particle sizes and shapes, predominantly tiny agglomerated particles. Elemental analysis confirmed the presence of chromium (Cr), selenium (Se), and trace elements, likely originating from the substrate composition.

REFERENCES

1. Aboud A.A., Mukherjee A., Revaprasadu N., Mohamed A.N. J. Mater. Res. Technol., 2019, 8:2021.
2. Akhtar M., Malik M.A., Raftery J., O'Brien P. J. Mater. Chem. A, 2014, 2:20612 [Crossref], [Google Scholar], [Publisher] [27]. Obata Y., Karateev I.A., Pavlov I., Vasiliev A.L., Haindl S. Micromachines, 2021, 12:1224.
3. Arunkumar, K. D., Valanarasu, S., Ganesh, V., Shkir, M., Al-Faify, S., & Algarni, H. (2018). Effect of potential voltages on key functional properties of transparent
4. Augustine C., Nnabuchi M., Chikwenze R., Anyaegbunam F., Kalu P., Robert B., Nwosu C., Dike C., Taddy E. MRX, 2019, 6:066416.AZO thin films prepared by electrochemical deposition method for optoelectronic applications. Journal of Materials Research, 33(11), 1523–1533.
5. Contreras-Rodriguez R., MendivilReynoso T., Landin I.O., Castillo S., OchoaLandín R. ACS omega, 2023, 8:41411.
6. Egwunyenga N., Onuabuchi V., Okoli N., Nwankwo I. IRJMT, 2021, 3:1.
7. Egwunyenga N., Ezenwaka L., Ezenwa I., Okoli N. MRX, 2019, 6:105921.
8. Elekalachi C., Ezenwa I., Okereke A., Okoli N., Nwori A. Nanoarchitectonics, 2023, 26.
9. Eze C., Ezenwa I., Okoli N., Elekalachi C., Okereke N. J. Nano Mater. Sci. Res., 2023, 2:123.
10. Hussain R.A., Badshah A., Younis A., Khan M.D., Akhtar J. Thin Solid Films, 2014, 567:58.
11. Ijeh R.O., Ugwuoke C.O., Ugwu E.B., Aisida S.O., Ezema F.I. Ceram. Int., 2022, 48:4686.
12. Kariper. I.A (2015). Optical and structural properties of Crse thin film with chemical bath deposition. journal of non-oxide glasses 7, (3) 37- 44. Erciyes University, Education Faculty, 38039, Kayseri, Turkey.
13. Kukay.A. (2019). Chromium selenide synthesis and characterization. Theses and Dissertations. 2467. https://commons.und.edu/theses/2467.
14. Kumar K.D.A., Valanarasu S., Ganesh V., Shkir M., AlFaify S., Algarni H. J. Mater. Res., 2018, 33:1523.
15. Matthews, P. D., McNaughter, P. D., Lewis, D. J. and Paul O'Brien, P. (2017). Shining a Light on Transition Metal Chalcogenides for Sustainable Photovoltaics. Chemical Science, 8(6): 4177 –4187.
16. Muogbo, I.P, Ekpunobi, A.j. and Okoli, N.L. (2023). Journal of Medicinal and Nanomaterials Chemistry 4 (2023) 307-322.
17. Nwori A.N., Ezenwaka L.N., Ottih I.E., Okereke N.A., Okoli N.L. Trends Sci., 2022, 19:5747.
18. Nkele A.C., Nwankwo U., Alshoaibi A., Ezema F.I. Results Opt., 2023, 13:100521.
19. Okoli N.L., Ezenwaka L.N., Okereke N.A., Ezenwa I.A., Nwori N.A. Trends Sci, 2022, 19:5686.
20. Olubosede O., Faremi A.A., Owolabi F.M., Ajiboye E., Fateye J.O., Olanibi E.O. FUOYE J. Eng. Technol., 2020, 5:74.
21. Onu C.P., Ekpunobi A.J., Okafor C.E., Ozobialu L.A. Asian J. Res. Rev. Phy., 2023, 7:17.

22. Pesko E., Zukowska G., Zero E., KrztonMaziopa A. Thin Solid Films, 2020, 709:138121.
23. Ramaraj, S., Mani, S., Chen, S.-M., Palanisamy, S., Velusamy, V., Hall, J. M., Chen. T.-W. and Tseng, T. W. (2018). Hydrothermal Synthesis of Cr_2Se_3 Hexagons for Sensitive and Low-level Detection of 4-Nitrophenol in Water. Scientific Reports, 8(1), 1-9.
24. Roy A., Dey R., Pramanik T., Rai A., Schalip R., Majumder S., Guchhait S., Banerjee S.K. Phys. Rev. Mater., 2020, 4:025001.
25. Salim H., Olusola O., Ojo A., Urasov K., Dergacheva M., Dharmadasa I. J. Mater. Sci. Mater. Electron., 2016, 27:6786.
26. Saravanan V., Anusuya M., Ugwuoke C.O., Nwulu N., Ezema F.I. Results Opt., 2023, 13:100548.
27. Savjani, N., Lewis, E. A., Pattrick, S. J. Haigh and O'Brien. P. (2014). MoS_2 nanosheet production by the direct exfoliation of molybdenite minerals from several type-localities Royal Society of Chemistry Advance, 4, 35609–35613.
28. Tauc J., Grigorovici R., Vancu A. physica status solidi (b), 1966, 15:627.
29. Thanikaikarasan S., Perumal R., Thanikaivelan E., Ahamad T., Alshehri S.M. J. New Mater. Electrochem. Syst., 2023, 26:101.
30. Whyte G., Awada C., Offor P., Whyte F., Kanoun M., Goumri-Said S., Alshoaibi A., Ekwealor A., Maaza M., Ezema F.I. J. Alloys Compd., 2021, 855:157324.
31. Zeynalova A.O., Javadova S.P., Majidzade V.A., Sh A.A. 2021, 262.